

## Supplementary Material Cover Sheet

### Transport of tetracycline in saturated porous media: combined functions of inorganic ligands and solution pH

Qiqi Wei <sup>1</sup>, Qiang Zhang <sup>2</sup>, Yihan Jin <sup>1</sup>, Usman Farooq <sup>1</sup>, Weifeng Chen <sup>3</sup>,

Taotao Lu <sup>4</sup>, Deliang Li <sup>1,\*</sup>, and Zhichong Qi <sup>1,\*\*</sup>

<sup>1</sup> Henan Joint International Research Laboratory of Environmental Pollution Control Materials, College of Chemistry and Chemical Engineering, Henan University, Kaifeng 475004, China

<sup>2</sup> Ecology institute of the Shandong academy of sciences, Qilu University of Technology (Shandong Academy of Sciences), Jinan 250353, China

<sup>3</sup> Key Laboratory for Humid Subtropical Eco-geographical Processes of the Ministry of Education/ Fujian Provincial Key Laboratory for Plant Eco-physiology/ School of Geographical Sciences, Fujian normal university, Fuzhou, Fujian 350007, China

<sup>4</sup> College of Water Resources & Civil Engineering, Hunan Agricultural University, Changsha 410128, China

Manuscript prepared for *Environmental Science: Processes & Impacts*

\* Corresponding author: Deliang Li (lideliang@henu.edu.cn)

\*\* Corresponding author: Zhichong Qi ([qizhichong1984@163.com](mailto:qizhichong1984@163.com)).

Number of pages: 25

Number of tables: 5

Number of figures: 10

### **S1. Determine of the $\zeta$ -potential of the sand grains**

The zeta potential of sand grains was measured by using a Zeta-Plus potential analyzer (Zetasizer nano ZS90, Malvern Instruments, UK) at room temperature (25°C) according to the method described in previous studies.<sup>S1</sup> It should be noted that, because the sand grains were too large for direct measurement by the zeta potential analyzer, a few sand grains were crushed into fine powders and then mixed with the appropriate chemistry solution (see Table 1) in an ultrasonic bath for 30 min. Then, the mixture was formed a sufficiently stable suspension that could be used for zeta potential measurement.

## **S2. Determination of the CEC of quartz sand**

The cation exchange capacity (CEC) of sand was measured by the following the previously reported method.<sup>S2</sup> In brief, 500 mL of CaCl<sub>2</sub> (1eq/L) are injected from bottom to top through a column filled with 10 g of sand. Then, 150 mL of CaCl<sub>2</sub> (0.05 eq/L) is injected followed by 500 mL of KNO<sub>3</sub> (1eq/L). The percolate is collected in 500 mL flask and the total calcium was titrated with EDTA (0.02eq/L) at pH 12 using the Eriochrome Black T as indicator. At the same time, the chloride is titrated with AgNO<sub>3</sub> (0.05eq/L) using the K<sub>2</sub>CrO<sub>4</sub> as indicator. The CEC is given by:

$$\text{CEC (meq /100g)} = 2v-5V$$

where  $v$  is the volume (mL) of EDTA required for calcium titration and  $V$  the volume (mL) of AgNO<sub>3</sub> required for chlorides titration.

### S3. Calculation of porosity

The porosity of sand columns was measured gravimetrically.<sup>S3</sup> The detailed equation is as follows:

$$\text{porosity} = \frac{V_c - V_s}{V_c} = \frac{V_c - \frac{m_{\text{sand}}}{\rho_{\text{sand}}}}{V_c}$$

Where  $V_c$  (cm<sup>3</sup>) is the volume of column,  $V_s$  (cm<sup>3</sup>) is the volume of sand in the column,  $m_{\text{sand}}$  (g) is the mass of sand in the column and  $\rho_{\text{sand}}$  (g/cm<sup>3</sup>) is the real density of sand (2.65 g/cm<sup>3</sup>).<sup>S4,S5</sup>

#### **S4. Procedures used to obtain the retention profiles of tetracycline in the column**

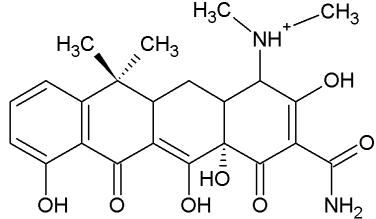
To obtain the retention profiles of tetracycline in the column at the end of the transport experiments, the sand columns were dissected into 10 layers of 1.0 cm segments and subsequently re-entrained to DI water, then vibrated on a horizontal motion shaker for 24 h at the ambient temperature. Then the vials were centrifuged at 5000 rpm for 20 min, and the supernatants were withdrawn to measure the concentrations of tetracycline. The sand segments were oven-dried at 90 °C overnight to obtain the dry weight of the sand in each segment.

## **S5. Adsorption of inorganic ligands onto sand grains**

Adsorption experiments were also conducted to determine the adsorbed amount of inorganic ligands onto sand grains under different pH conditions. The initial concentrations of inorganic ligands in the 20-mL amber glass vial were 0.5 mM; and the initial mass of sand grains was 5 g. The vials were mixed and then left on an orbital shaker operated at room temperature for 12 h (the duration equal to the transport experiment). The liquid and solid phases were separated by centrifugation at 5000 rpm for 30 min, and then the supernatants were filtered through 0.45  $\mu\text{m}$  filtering membrane. The concentration of iodate in the supernatant was determined by the method of Dai et al.<sup>S6</sup>. Briefly, iodate was reduced to iodide by 1% Vc (ascorbic acid), and was determined by Ion Chromatography (Dionnex 600, USA). The concentration of silica in the solution was determined by colorimetry with ammonium molybdate. The absorbance of the solution was measured with a UV/Vis spectrophotometer at 385 nm.<sup>S7</sup> The concentration of phosphate in the supernatant was determined by using the colorimetric technique.<sup>S8</sup> Briefly, 0.06 mL of 11 N  $\text{H}_2\text{SO}_4$  was added to 3 mL of the supernatant, followed by the addition of 0.24 mL of 8 g/L ammonium molybdate and 0.2 g/L antimony potassium tartrate (Sigma-Aldrich). The resulting solution was mixed to allow for the formation of an antimony-phospho-molybdate complex. Next, 0.12 mL of 60 g/L ascorbic acid (Sigma-Aldrich) was added to the solution to reduce the complex to a blue-colored complex. The absorbance of the solution was measured with a UV/Vis spectrophotometer at 650 nm. The adsorbed inorganic ligand (iodate, silicate, or

phosphate) was then determined by the difference between the initial and final phosphate concentrations in the aqueous phase. All experiments were run in triplicate.

**Table S1.** Selected properties of tetracycline.

Antibiotics	Molecular formula	Chemical structure	Molecular weight (g/mol)	Log $K_{ow}$ <sup>a</sup>	$pK_a$ <sup>b</sup>	Solubility (mol/L)
tetracycline	$C_{22}H_{24}N_2O_8$		444.43	-1.30	$pK_{a1}=3.32$ $pK_{a2}=7.78$ $pK_{a3}=9.58$	0.041

<sup>a</sup> Derived from Daghrir and Drogui.<sup>S9</sup><sup>b</sup> Derived from Li et al..<sup>S10</sup>



**Table S2.**  $\zeta$ -potentials (mV) of quartz sand under different conditions.

No.	Porous media	ligand	TC conc. (mg/L)	electrolyte solution	pH	$\zeta$ -potentials (mV)
1	quartz sand	0	3	10 mM NaCl	5.0	-75.6 $\pm$ 2.3
2	quartz sand	0	3	10 mM NaCl	7.0	-79.1 $\pm$ 1.2
3	quartz sand	0	3	10 mM NaCl	9.0	-82.5 $\pm$ 1.5
4	quartz sand	0.5 mM iodate	3	10 mM NaCl	5.0	-78.7 $\pm$ 2.1
5	quartz sand	0.5 mM silicate	3	10 mM NaCl	5.0	-79.9 $\pm$ 2.0
6	quartz sand	0.5 mM phosphate	3	10 mM NaCl	5.0	-82.6 $\pm$ 0.7
7	quartz sand	0.5 mM iodate	3	10 mM NaCl	7.0	-79.5 $\pm$ 1.6
8	quartz sand	0.5 mM silicate	3	10 mM NaCl	7.0	-82.8 $\pm$ 0.7
9	quartz sand	0.5 mM phosphate	3	10 mM NaCl	7.0	-84.1 $\pm$ 1.3
10	quartz sand	0.5 mM iodate	3	10 mM NaCl	9.0	-85.3 $\pm$ 1.5
11	quartz sand	0.5 mM silicate	3	10 mM NaCl	9.0	-87.6 $\pm$ 0.9
12	quartz sand	0.5 mM phosphate	3	10 mM NaCl	9.0	-89.3 $\pm$ 1.1

**Table S3.** Sorption isotherm parameters of TC onto sand grains under different solution chemistry conditions.

No.	electrolyte solution	surfactants	pH	Freundlich model		
				$K_F$ (mg <sup>1-n</sup> L <sup>n</sup> /kg)	$n$	$R^2$
1	10 mM NaCl	/	5.0	8.335 ± 0.152	0.642 ± 0.023	0.992
2	10 mM NaCl	/	7.0	6.998 ± 0.239	0.723 ± 0.016	0.996
3	10 mM NaCl	/	9.0	4.934 ± 0.215	0.753 ± 0.012	0.992
4	10 mM NaCl	0.5 mM iodate	5.0	5.824 ± 0.321	0.621 ± 0.011	0.994
5	10 mM NaCl	0.5 mM silicate	5.0	5.969 ± 0.151	0.806 ± 0.025	0.993
6	10 mM NaCl	0.5 mM phosphate	5.0	3.697 ± 0.103	0.803 ± 0.008	0.997
7	10 mM NaCl	0.5 mM iodate	7.0	5.196 ± 0.127	0.694 ± 0.017	0.991
8	10 mM NaCl	0.5 mM silicate	7.0	4.526 ± 0.269	0.664 ± 0.020	0.985
9	10 mM NaCl	0.5 mM phosphate	7.0	2.507 ± 0.133	0.857 ± 0.019	0.993
10	10 mM NaCl	0.5 mM iodate	9.0	2.933 ± 0.459	0.801 ± 0.039	0.983
11	10 mM NaCl	0.5 mM silicate	9.0	2.507 ± 0.143	0.857 ± 0.011	0.993
12	10 mM NaCl	0.5 mM phosphate	9.0	2.350 ± 0.387	0.788 ± 0.041	0.986

**Table S4.** Adsorption amount of inorganic ligands onto sand. Error bars represent standard deviations from replicate experiments (n=3)

ligand	electrolyte solution	pH	$q$ (mmol-ligands/kg-sand)
0.5 mM iodate	10 mM NaCl	5.0	$0.27 \pm 0.02$
0.5 mM silicate	10 mM NaCl	5.0	$0.12 \pm 0.05$
0.5 mM phosphate	10 mM NaCl	5.0	$1.76 \pm 0.12$
0.5 mM iodate	10 mM NaCl	7.0	$0.19 \pm 0.03$
0.5 mM silicate	10 mM NaCl	7.0	$0.58 \pm 0.11$
0.5 mM phosphate	10 mM NaCl	7.0	$1.53 \pm 0.02$
0.5 mM iodate	10 mM NaCl	9.0	$0.13 \pm 0.01$
0.5 mM silicate	10 mM NaCl	9.0	$0.42 \pm 0.11$
0.5 mM phosphate	10 mM NaCl	9.0	$0.77 \pm 0.05$

**Table S5.** Parameters of the pseudo-second-order models for adsorption of TC with or without inorganic ligand onto sand grains (the initial concentration of TC was 3 mg/L, the mass of sand was 5 g, the initial concentration of inorganic ligand was 0.5 mM, pH 7.0, and the temperature was 298 K). Error bars represent standard deviations of triplicate samples (each with  $p < 0.05$ ).

No.	Background solution	Pseudo-second-order kinetic model		
		$k_2$ (kg/(mg·h))	$k_0$ ( $k_2q_e^2$ ) <sup>a</sup> (mg/(kg·h))	$R^2$
1	10 mM NaCl	0.034 ± 0.007	0.75 ± 0.02	0.991
2	10 mM NaCl + 0.5 mM iodate	0.043 ± 0.009	0.70 ± 0.05	0.993
3	10 mM NaCl + 0.5 mM silicate	0.047 ± 0.011	0.67 ± 0.09	0.995
4	10 mM NaCl + 0.5 mM phosphate	0.049 ± 0.005	0.65 ± 0.03	0.997

<sup>a</sup>  $k_0$  refers to the initial sorption rate,  $k_0 = k_2q_e^2$ .

**Table S6.** Fitted parameters of two-site nonequilibrium transport model from breakthrough results of column experiments.

Column No.	ligands	electrolyte solution	pH	Parameters of two-site nonequilibrium transport model						
				$R$ (-)	$\beta$ (-)	$\omega$ (-)	$f$ (-)	$\alpha$ (1/d)	$K_d$ (L/kg)	$r^2$
1	0	10 mM NaCl	5.0	$2.52 \pm 0.05$	$0.526 \pm 0.012$	$0.421 \pm 0.015$	$0.213 \pm 0.007$	$5.94 \pm 0.21$	$0.53 \pm 0.07$	0.999
2	0	10 mM NaCl	7.0	$2.34 \pm 0.12$	$0.574 \pm 0.008$	$0.308 \pm 0.012$	$0.257 \pm 0.012$	$5.20 \pm 0.15$	$0.47 \pm 0.11$	0.998
3	0	10 mM NaCl	9.0	$1.79 \pm 0.15$	$0.692 \pm 0.015$	$0.167 \pm 0.021$	$0.293 \pm 0.011$	$5.09 \pm 0.23$	$0.28 \pm 0.03$	0.998
4	0.5 mM iodate	10 mM NaCl	5.0	$2.05 \pm 0.09$	$0.612 \pm 0.011$	$0.268 \pm 0.016$	$0.301 \pm 0.025$	$5.50 \pm 0.08$	$0.39 \pm 0.05$	0.997
5	0.5 mM silicate	10 mM NaCl	5.0	$2.39 \pm 0.12$	$0.544 \pm 0.003$	$0.380 \pm 0.025$	$0.226 \pm 0.007$	$5.59 \pm 0.35$	$0.51 \pm 0.06$	0.998
6	0.5 mM phosphate	10 mM NaCl	5.0	$1.83 \pm 0.06$	$0.702 \pm 0.023$	$0.171 \pm 0.007$	$0.340 \pm 0.029$	$5.15 \pm 0.27$	$0.35 \pm 0.02$	0.999
7	0.5 mM iodate	10 mM NaCl	7.0	$2.30 \pm 0.03$	$0.581 \pm 0.025$	$0.274 \pm 0.009$	$0.258 \pm 0.023$	$4.65 \pm 0.25$	$0.46 \pm 0.07$	0.996
8	0.5 mM silicate	10 mM NaCl	7.0	$2.02 \pm 0.11$	$0.635 \pm 0.009$	$0.206 \pm 0.013$	$0.275 \pm 0.001$	$4.59 \pm 0.27$	$0.39 \pm 0.05$	0.998
9	0.5 mM phosphate	10 mM NaCl	7.0	$1.56 \pm 0.07$	$0.745 \pm 0.016$	$0.108 \pm 0.002$	$0.296 \pm 0.005$	$4.42 \pm 0.16$	$0.21 \pm 0.01$	0.997
10	0.5 mM iodate	10 mM NaCl	9.0	$1.75 \pm 0.09$	$0.721 \pm 0.013$	$0.137 \pm 0.008$	$0.349 \pm 0.008$	$4.45 \pm 0.15$	$0.27 \pm 0.03$	0.996
11	0.5 mM silicate	10 mM NaCl	9.0	$1.65 \pm 0.07$	$0.773 \pm 0.026$	$0.102 \pm 0.007$	$0.424 \pm 0.036$	$4.36 \pm 0.11$	$0.25 \pm 0.03$	0.993
12	0.5 mM phosphate	10 mM NaCl	9.0	$1.51 \pm 0.05$	$0.812 \pm 0.031$	$0.067 \pm 0.002$	$0.446 \pm 0.031$	$3.86 \pm 0.09$	$0.19 \pm 0.02$	0.995

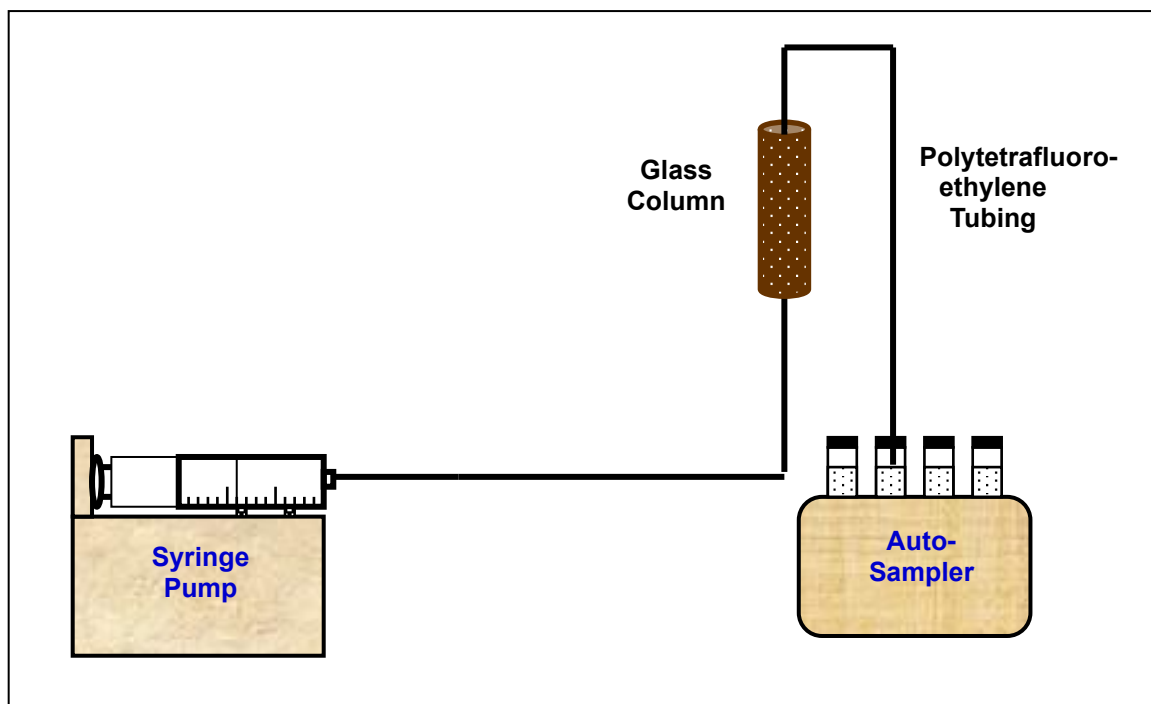


**Fig. S1** Schematic illustration of experimental apparatus of column tests.

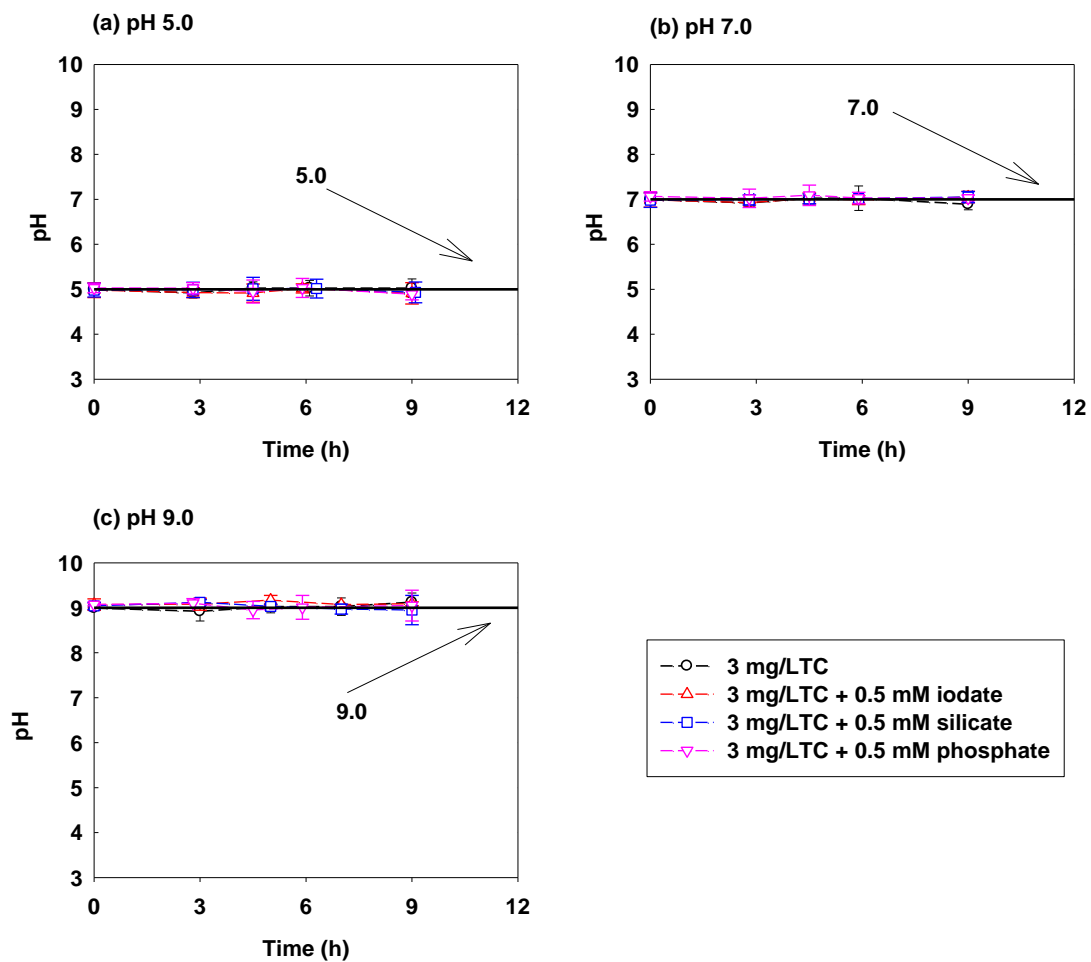


**Fig. S2.** The change of pH values in influents under different conditions during TC mobility: (a) pH 5.0; (b) pH 7.0; and (c) pH 9.0.

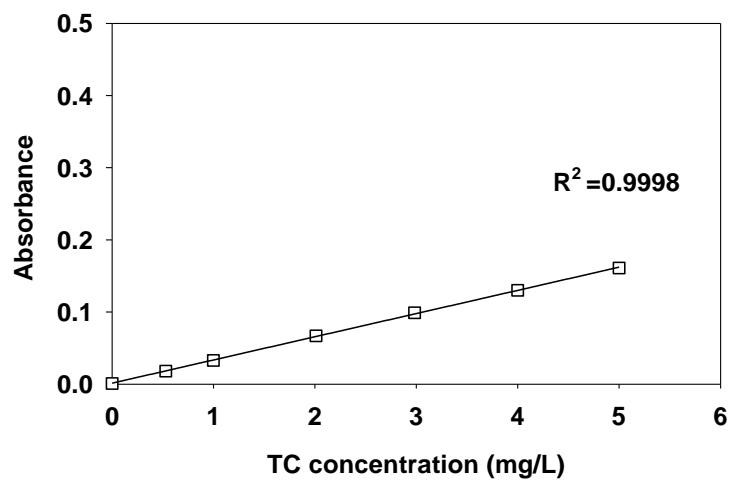


**Fig. S3.** Calibration curve as absorbance at the wavelength of 360 nm vs. concentration of TC in solution.



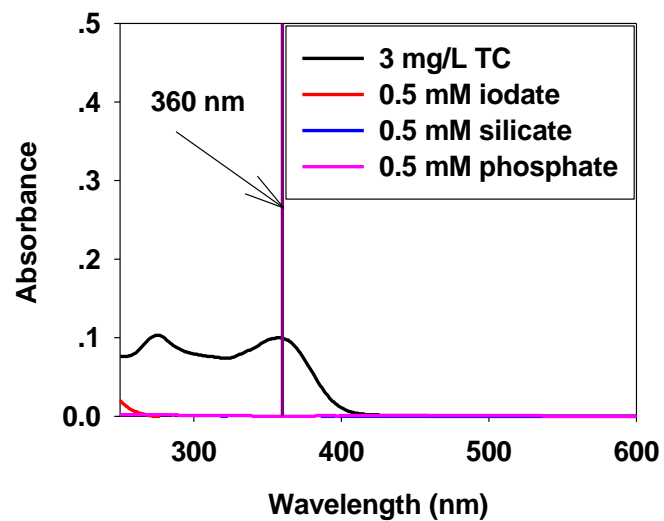


**Fig. S4.** UV/Vis spectra of TC (3 mg/L) in the absence and presence of inorganic ligands.

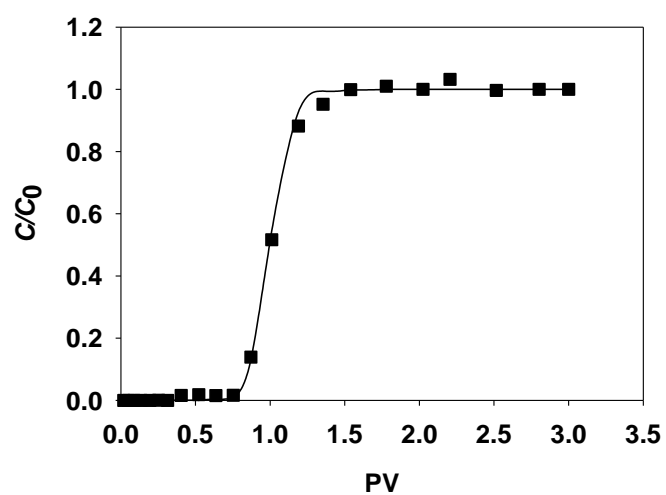


**Fig. S5.** Representative breakthrough curve of conservative tracer ( $\text{Br}^-$ ). The line was plotted by fitting the breakthrough data with the one-dimensional steady-state advection-dispersion equation.

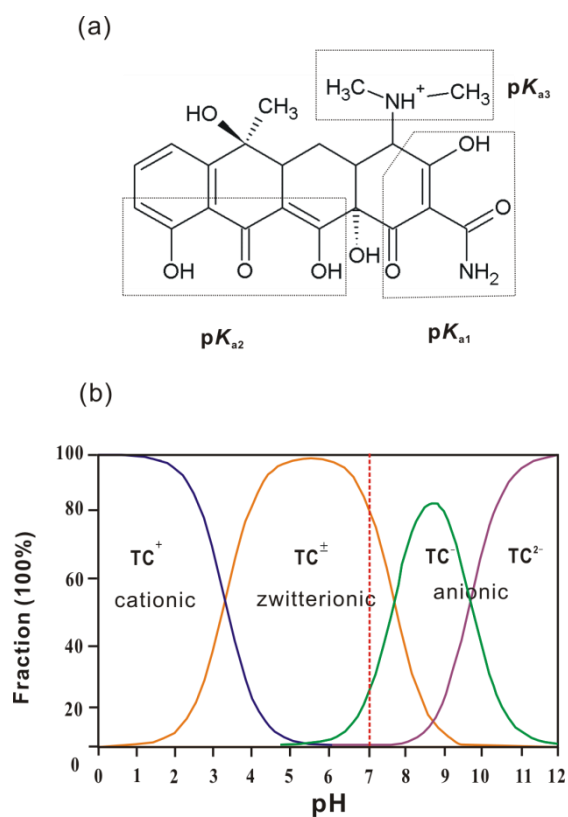


**Fig. S6.** (a) Structure of tetracycline (TC). The regions framed by dashed lines represent the three functional groups associated with the corresponding acidic dissociation constants ( $pK_a$ ); and (b) pH-dependent speciation of the whole tetracycline molecular and the functional groups, respectively.

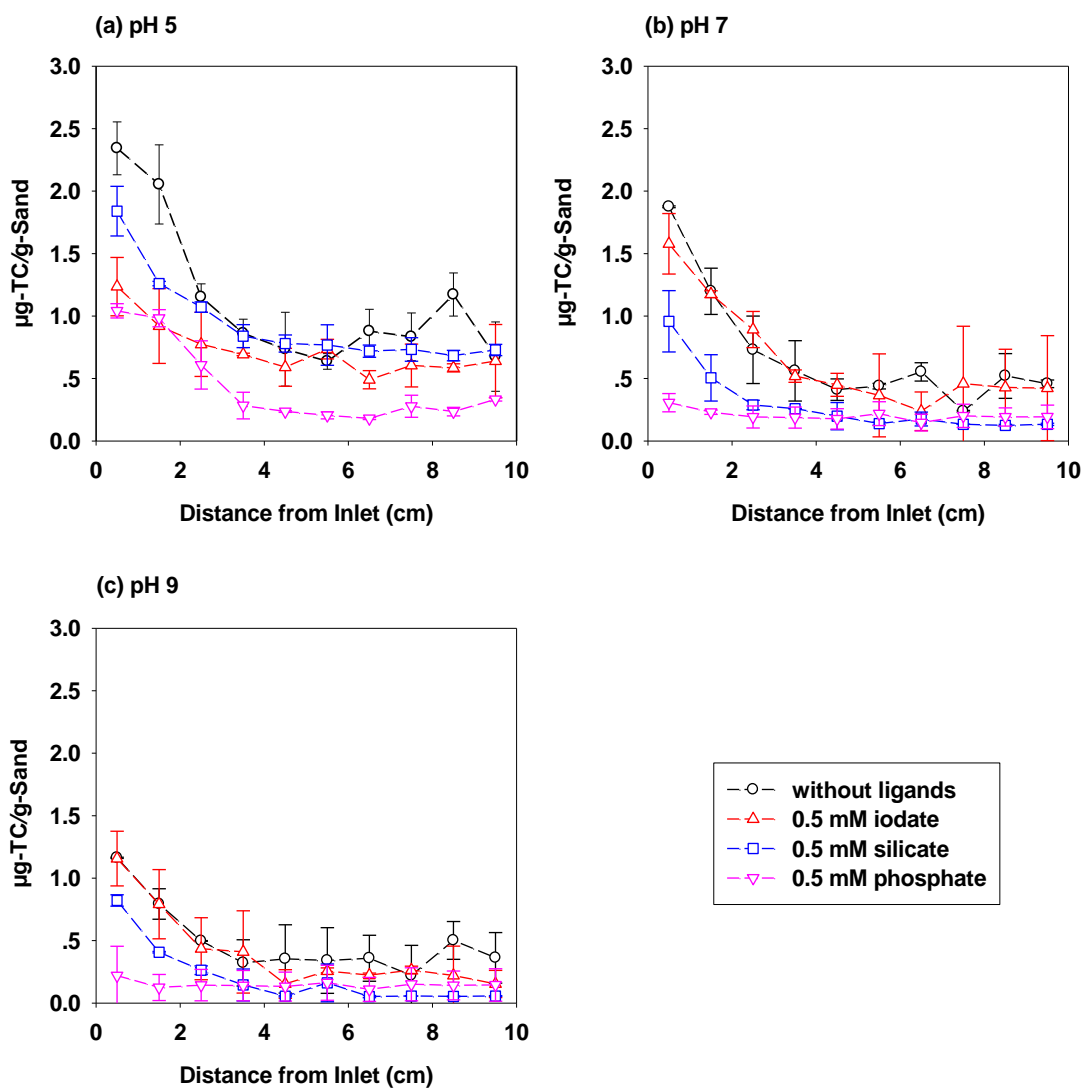


**Fig. S7.** Retained profiles of TC in the presence of inorganic ligands at different pH conditions: (a) pH 5 (columns 1, 4–6, Table 2), (b) pH 7 (columns 2, 7–9, Table 2), and (c) pH 9 (columns 3, 10–12, Table 2).

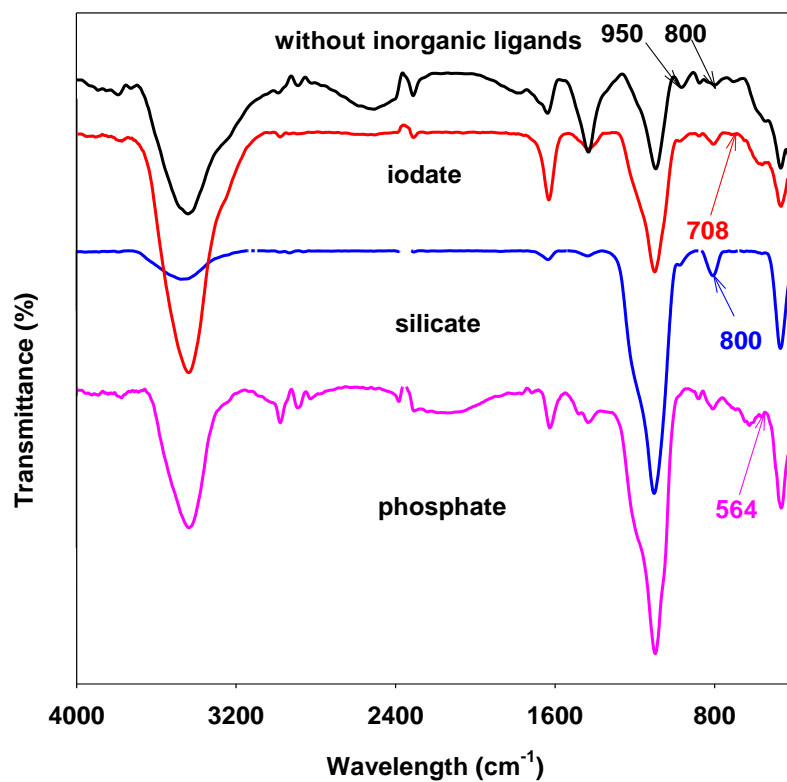


**Fig. S8.** Fourier transform infrared (FTIR) spectra of quartz sand with or without inorganic ligands. The peaks at  $950\text{ cm}^{-1}$  and  $800\text{ cm}^{-1}$  could be assigned to the Si–OH and Si–O–Si in sand;<sup>S11</sup> the absorption band centered at  $708\text{ cm}^{-1}$  is indicative of iodate group;<sup>S12</sup> the peaks at  $564\text{ cm}^{-1}$  could be assigned to the O–P–O asymmetric vibration.<sup>S13</sup>

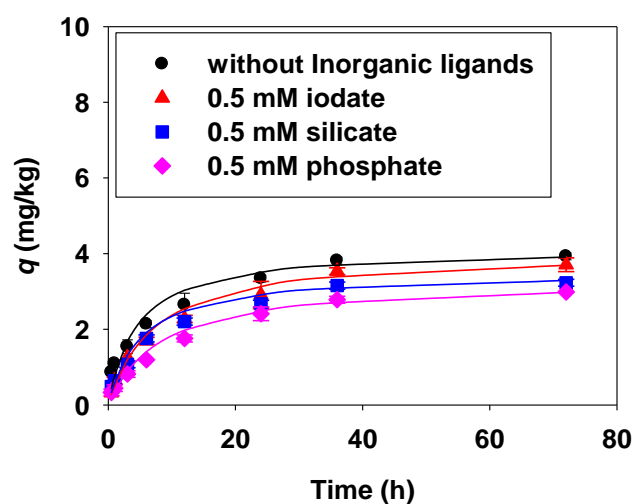


**Fig. S9.** Adsorption kinetics of TC with or without inorganic ligands onto sand grains at 10 mM NaCl (pH 7.0). The solid lines were plotted by curve fitting the data using pseudo-second-order kinetic model.  $m_{\text{sand}} = 5$  g, and the initial concentration of TC was 3 mg/L. Error bars represent standard deviations of triplicate samples (each with  $p < 0.05$ ).

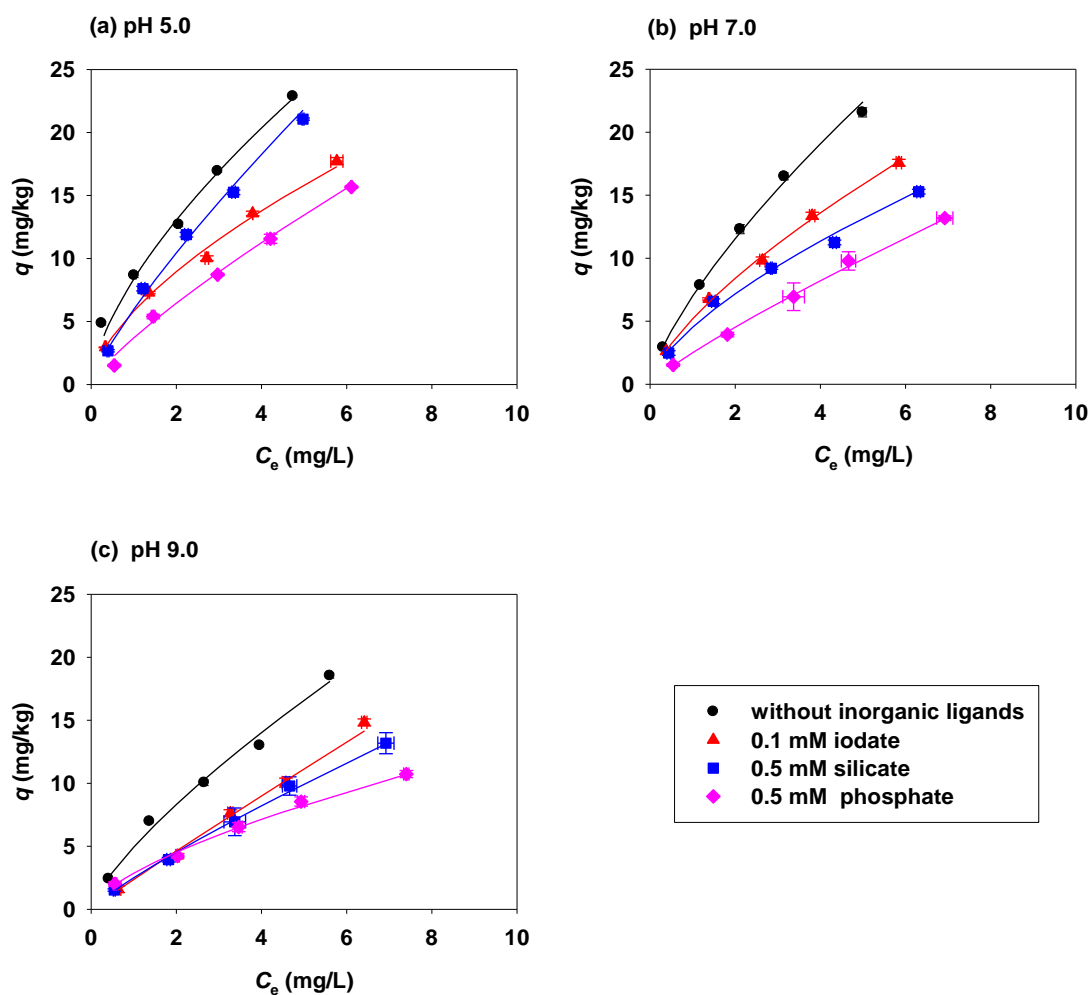


**Fig. S10.** Effects of inorganic ligands on the adsorption of TC onto sand grains under different pH conditions: (a) pH 5.0; (b) pH 7.0; and (c) pH 9.0.  $C_e$  (mg/L) is the equilibrium aqueous concentration of TC;  $q$  (mg/g) is the concentration of TC adsorbed quartz sand.  $m_{\text{sand}} = 5$  g, and ionic strength was 10 mM NaCl. The solid lines on the panel are the Freundlich model fitting results. Error bars represent standard deviations of triplicate samples (each with  $p < 0.05$ ).

## References

- S1. P.N. Mitropoulou, V.I. Syngouna and C.V. Chrysikopoulos, Transport of colloids in unsaturated packed columns: role of ionic strength and sand grain size, *Chem. Eng. J.*, 2013, 232, 237–248.
- S2. M. Abdelwaheb, K. Jebali, H. Dhaouadi and S. Dridi-Dhaouadi, Adsorption of nitrate, phosphate, nickel and lead on soils: Risk of groundwater contamination, *Ecotox. Environ. Safe.*, 2019, 179, 182–187.
- S3. L. Li, C. Qian and Y. Zhao, Pore structures and mechanical properties of microbe-inspired cementing sand columns. *Int. J. Civ.Eng.*, 2014, 12, 207–212.
- S4. S. Kim, G.S. Lee, D. Kim, J. Hahn and W. H. Ryang, Variation of temperature-dependent sound velocity in unconsolidated marine sediments: laboratory measurements. *Mar. Georesour. Geote.* 2018, 36, 280–287.
- S5. S. Skuodis, A. Norkus, N. Dirgeliene and L. Rimkus, Determining characteristic sand shear parameters of strength via a direct shear test. *J. Civ. Eng. Manage.*, 2016, 22, 271–278.
- S6. J. Dai, M. Zhang and Y. Zhu, Adsorption and desorption of iodine by various chinese soils: I. Iodate, *Environ. Int.*, 2004, 30, 525–530.
- S7. M. Tanakaa and K. Takahashib, Silicate species in high ph solution molybdate, whose silica concentration is determined by colorimetry, *Anal. Chim. Acta*, 2001, 429, 117–123.
- S8. X. Liu and K.L. Chen, Aggregation and interactions of chemical mechanical planarization nanoparticles with model biological membranes: Role of phosphate adsorption, *Environ.Sci. Nano*, 2016, 3, 146–156.
- S9. R. Daghrir and P. Drogui, Tetracycline antibiotics in the environment: a review, *Environ. Chem. Lett.*, 2013, 11, 209–227.



- S10. J. Li, K. Zhang and H. Zhang, Adsorption of antibiotics on microplastics, *Environ.Pollut.*, 2018, 237, 460–467.
- S11. D. V. Quang, J. E. Lee, J. K. Kim, Y. N. Kim, G. N. Shao and H. T. Kim, A gentle method to graft thiol-functional groups onto silica gel for adsorption of silver ions and immobilization of silver nanoparticles, *Powder Technol.*, 2013, 235, 221 –227.
- S12. C. Q. Ning, Y. Greish and A. El-Ghannam, Crystallization behavior of silica-calcium phosphate biocomposites: XRD and FTIR studies, *J. Mater. Sci.* 2004, 15, 1227–1235.
- S13. Y. G. C. Q. Ning, A. El-Ghannam, Crystallization behavior of silica-calcium phosphate biocomposites: XRD and FTIR studies, *J. Mater. Sci.*, 2004, 15, 1227 –1235.